Vol.7 No.1 Jan 2024

Multimedia Research

Received 21 August, Revised 24 October, Accepted 15 November

Metaheuristic Assisted Deep Neural Network for Diabetic Mellitus Diagnosis via Proposed Texture Feature Descriptor

Phani Kulkarni

University of Missouri-Kansas City
MISSOURI, USA
kulkarniphani@gmail.com

Abstract: Diabetes mellitus (DM) indicates the group of metabolic disorders, which shares the hyperglycemia phenotype. The secondary pathophysiological changes are caused by the metabolic dysregulations related to DM in many organ systems that result in various difficulties liable for the mortality and morbidity linked with the disease. However, the early diagnosis of the disease is possible from the human tongue. Therefore, this work introduces a new DM diagnosis model that includes two major phases: (i) Feature extraction, and (ii) Classification. Initially, the input image is given to the feature extraction phase, in which the color feature, texture feature, and geometry features are extracted. The texture features include the Proposed Tri-region distance-based Local Binary Pattern (TRD-LBP) and Gray Level Co-occurrence Matrix (GLCM) features, whereas, the 13 geometry features are also included in this feature extraction phase. Subsequently, these extracted features are provided as the input to the Optimized Neural Network (NN), where the diagnosis takes place. To make the detection more precise, the training of NN is carried out by the Self Adaptive Particle Swarm Optimization (SAPSO) algorithm via tuning the optimal weights. Finally, the performance analysis is made among the adopted and the existing approaches for various measures like sensitivity, NPV, accuracy, FDR, specificity, FPR, precision, MCC, FNR, and F1-score, respectively.

Keywords: Diabetes Mellitus; Feature Extraction; Classification; Neural Network; Optimization.

Nomenclature

Abbreviation	Description
ADAM	Androgen Deficiency in Aging Male
ANC	Antenatal Care
ALR2	Aldose Reductase
CGM	Continuous Glucose Monitoring
CV	Coefficient of Variation
CNN	Convolutional Neural Network
CONGA	Continuous Overall Net Glycemic Action
DM	Diabetes Mellitus
DR	Diabetic Retinopathy
DT	Decision Tree
FT	Free Testosterone
FF	FireFly
GLCM	Gray Level Co-occurrence Matrix
GDM	Gestational Diabetes
IDM	Inverse Difference Moment
LBP	Local Binary Pattern
LBGI	Low Blood Glucose Index
LDA	Linear Discriminant Analysis
LR	Logistic Regression
LE	Lower-Extremity
ML	Machine Learning
MI	Motricity Index
NN	Neural Network
NIHSS	National Institutes of Health Stroke Scale
PTP1B	Protein Tyrosine Phosphatase 1B
PCA	Principal Component Analysis
PSO	Particle Swarm Optimization
PDB	Protein Databank
SHBG	Sex Hormone-Binding Globulin
SD	Standard Deviation
SVM	Support Vector Machine
SAPSO	Self Adaptive Particle Swarm Optimization
TRD-LBP	Tri-region distance based Local Binary Pattern
T2DM	Type 2 Diabetes Mellitus
TT	Total Testosterone

https://doi.org/10.46253/j.mr.v7i1.a4

1. Introduction

DM is a metabolic disease that particularly affects humans with increased blood sugar levels due to pancreas disorder with insufficient secretion of insulin. The complications of DM disease may affect every organ system in the human body [1] [2]. The timely prevention, treatment, and diagnosis must be done properly for those DM patients. Since, it avoids diabetes-related complications like retinopathy, neuropathy, nephropathy, stroke, death, and cardiovascular disease [3] [4]. Moreover, the above symptoms are avoided or delayed, only when the blood glucose, blood pressure, and lipids are maintained properly in normal conditions. The human body can maintain stable glucose concentrations. Normally, the blood sugar lies among the 3.5-6.7mmol/l during fasting, and it rarely exceeds 8mmol/l after the meal. Generally, no glucose is present in the urine; however, the normal threshold above the glucose that appears in the urine is 10mmol/l [6] [7].

The major cause of diabetes is a lack of awareness of people's food habits. Due to this reason, the count of diabetes patients is gradually rising in our country [8]. Hence, the researchers are trying to set up a medical device that could test more people for cardiovascular disease, and diabetic patients with retinal disorder [9] [10]. Due to the increased number of diabetes patients and the shortage of medical services in certain regions, patients with DR are unable to be detected and treated on time thereby missing the best care facilities [11] [12]. This potentially contributes to irreversible visual loss and even blindness. Particularly in the early stage of diabetic patients, the DR is identified and treated quickly, and then the process of deterioration is well managed and postponed [13]. The impact of manual interpretation highly depends on the experience of the clinician. Sometimes, misdiagnosis happens by inexperienced doctors.

Various ML and data mining approaches were used for the treatment, diagnosis, and prognosis of diabetes [18] [19]. According to their normal physical examination results, the ML helps the individuals to make a preliminary decision regarding DM and this can serve as a guide for doctors [20] [21]. The most important problems would be how to pick the correct features and the right classifier for the ML process [22] [23]. Different algorithms including conventional ML [27] [28] [29] approaches like SVM, DT, LR, and so on, have recently been used to predict diabetes [30] [31][24]. DT is one of the common methods of ML in the medical field, which has the power to classify the disease [25]. The NN [45] [39] [40] [41] is a common method of ML that improves performance in several aspects. Deep CNNs have been recognized as a great computer vision technique for the past ten years by suppressing all other existing methodologies of image analysis [14] [15][16]. For improving the performance of several ML techniques, the concept of optimization [46] [44] [43] [42] has been used in this field. The major contributions of the adopted model are given below:

- Proposes a new variant of LBP features under three different regions (pentagon, octagon, and heptagon region).
- Proposes a new SAPSO algorithm for training the NN model via selecting the optimal weights.

In this paper, section 2 describes the review of Diabetic Mellitus detection. The proposed diabetic mellitus diagnosis model is described in section 3. The feature extraction: color feature, texture feature, and geometric feature are portrayed in section 4. Diabetic mellitus diagnosis via an optimized neural network is portrayed in section 5. Section 6 depicts the optimal tuning of weights via an improved particle swarm optimization algorithm. Section 7 specifies the result and discussion. At last, the conclusion of the paper is given in section 8.

2. Literature Review

2.1 Related works

In 2020, Biswas *et al.* [1] presented the hypogonadism prevalence between Indian men without and with T2DM with different metabolic parameters. Moreover, the albumin, SHBG, and TT levels in serum were calculated by the FT level. Further, the patients with an ADAM questionnaire and FT level greater than 6.35 ng/dL were diagnosed with hypogonadism. Lastly, the outcomes of the proposed work have shown higher prevalence in patients with T2DM.

In 2020, Rukiye *et al.* [2] investigated whether the oat ß-glucan and the supplemental soluble fiber affected controlling the variability and glycemic with DM type 1. Moreover, the work has included 3 phases and it was executed in 30 adolescents with type 1 DM. A standardized diet program was followed by every subject at Phase I, and the continuous standardized program was based on diet and the extra natural oat flakes in both Phase III, and II, respectively. In the end, the experimental outcomes of the

proposed work have achieved minimum levels of LBGI, SD, CONGA, and CV levels in phase III when compared to other Phases.

In 2020, Kusnanto *et al.* [3] determined type 2 DM to explore diabetes resilience among adults based on their qualitative study. By the snowball sampling process, 15 participants with T2DM were employed. The diabetes resilience indicators were the correct management of drugs, stress, diet, and activity. Moreover, the interview outlines were used for the data collection by the in-depth interview. At last, the outcomes of the adopted scheme have proven better resilience and higher prevalence than other existing schemes.

In 2020, Kolle *et al.* [4] determined the postprandial CGM data patterns for detection. For recognizing the postprandial patterns, the binary classifiers were trained to estimate the glucose rate in CGM data appearance. Further, the moving horizon estimation would determine the appearance rate on a simple process. Nevertheless, the LDA was used in the process of classification. When compared to threshold-based work, the proposed LDA has shown better sensitivity. The horizon classification has also shown the betterment of the proposed model for the low rate of false alarms.

In 2020, Antonios *et al.* [5] suggested the protein tyrosine phosphatase 1B inhibitors and aldose reductase used for the therapeutic approach in DM patients. In addition, the conventional models have been used in the X-ray crystal structures taken from PDB. Moreover, the proposed inhibitors were the best treatment for diabetes-associated pathologies and hyperglycemia instead of the therapeutic options for type 2 DM. Finally, the adopted method achieved better control of hyperglycemia and successful treatment than other existing models.

In 2020, Brian *et al.* [6] conducted a metabolomics study to determine the analytical models to identify the accurate predictors of gestational DM. Moreover, the 92 gravidas (i.e.), 46 control group, and 46 gestational DM group were included in the nested observational case-control study during the early pregnancy, in which it was matched through the gestational age at urine collection, body mass index, and maternal age. Based on the community standards, gestational DM was diagnosed. The classifier results have shown 96.7% accuracy in predicting GDM.

In 2020, Masafumi *et al.* [7] determined the pre-stroke comorbidities and the pre-stroke sarcopenia risk relationships cross-sectional study of MI. Furthermore, the analysis of multivariate regression would investigate the MI with sarcopenia risk relationship, comorbidities in these patients, and neurological deficit by the NIHSS. Finally, it was proved that the assessment might help the clinician.

In 2020, Achenef *et al.* [8] examined the gestational DM effects in Ethiopia based on the risks of adverse neonatal resultants. Moreover, the diagnosis of Gestational DM was done using the tolerance test strategy in 2 hours for 75g oral glucose within the latest criterion. For identifying the gestational DM effects based on the difficulties of adverse neonatal results, the multivariable log-binomial approach was used. Finally, the outcomes of the proposed model have attained improved neonatal outcomes than other existing models.

2.2 Review

Table I shows the review on DM detection. Initially, chi-square analysis was deployed in [1], which improves the parameters of body composition, better cardiovascular outcomes, best glycaemic control, and low serum FT level; however, based on certain feasibility constraints, the testosterone measurement was performed only once. The carbohydrate count method is exploited in [2] that offers a reduction of amplitude, reduced hyperglycemic and hypoglycemic fluctuations, and low frequency, but no modifications were done in the insulin doses. Moreover, the triangulation method was deployed in [3] that offers better resilience and higher prevalence. Nevertheless, health educations were not developed based on the local culture for improving diabetes resilience. Likewise, LDA was exploited in [4], which improves glucose regulation, low rate of false alarms, and higher sensitivity. However, the safety and robustness of meal detection were not improved using the voting system. Scaffold hopping approaches were exploited in [5] that eliminate the chance of adverse reactions and better control of hyperglycemia; however, the PTP1B and dual ALR2 inhibitors were not considered for the proper treatment of type II DM. In addition, an advanced analytical method is introduced in [6], which offers a high proportion, reduced fetal epigenetic disruptions, less perinatal morbidity, and reduced GDM prevalence. However, for validation and a separate training process, the study size was insufficient. MI method is suggested in [7] that offers reliability and avoids fatigue effects. However, the factors that influence the LE muscle strength with acute stroke were not considered in elderly patients. Finally, the Multivariable log-binomial model was implemented in [8], which improves the neonatal outcomes and better performance, but in the various phases of pregnancy, the repeated measurement of ANC indicators was not specified. Such limitations have to be taken into account based on DM detection in the present work effectively.

Table 1. *Review on conventional DM detection using various techniques: Features and Challenges*

Author [citation]	Adopted scheme	Features	Challenges
Biswas *et al.* [1]	chi-square analysis	✓ Improvement in parameters of body composition. ✓ Best glycaemic control ✓ Low serum FT level	❖ Based on certain feasibility constraints, the testosterone measurement was performed only once.
Rukiye *et al.* [2]	Carbohydrate count method	✓ Reduction of amplitude ✓ Reduce hyperglycemic and hypoglycemic fluctuations. ✓ Low frequency	❖ No modifications were made to the insulin doses.
Kusnanto *et al.* [3]	Triangulation method	✓ Better resilience ✓ Higher prevalence	❖ The health educations were not developed based on the local culture for improving diabetes resilience.
Kolle *et al.* [4]	LDA method	✓ Low rate of false alarms ✓ Improve the glucose regulation. ✓ Higher sensitivity	❖ The safety and robustness of meal detection were not improved using the voting system.
Antonios *et al.* [5]	Scaffold hopping approaches	✓ Successful treatment ✓ Better control of hyperglycemia. ✓ Eliminates the adverse reaction chances.	❖ The PTP1B and dual ALR2 inhibitors were not considered for the proper treatment of type II DM.
Brian *et al.* [6]	Advanced analytical methods	✓ Reduces GDM prevalence ✓ High proportion ✓ Reduced fetal epigenetic disruptions. ✓ Less perinatal morbidity	❖ For validation and a separate training process, the study size was insufficient.
Masafumi *et al.* [7]	MI method	✓ Reliable ✓ Avoid fatigue effects	❖ The factors that influence the LE muscle strength with acute stroke were not considered in elderly patients.
Achenef *et al.* [8]	Multivariable log-binomial model	✓ Improved neonatal outcomes. ✓ Better performance	❖ During various phases of pregnancy, the repeated measurement of ANC indicators was not specified.

3. Proposed Diabetic Mellitus Diagnosis Model

3.1 Proposed Architecture

This paper introduces a novel DM diagnosis model that consists of two major phases: (i) Feature extraction and (ii) Classification. Initially, the given tongue images are preprocessed under automatic segmentation that separates the foreground pixels from the background. Subsequently, the preprocessed image is given to the feature extraction phase, in which the color feature, texture feature, and geometry features are extracted. The texture features include proposed TRD-LBP and GLCM features; whereas, the geometry features include the 13 features like "length, area, width, center distance, length-width ratio, smaller-half-distance, square area ratio, triangle area, circle area, triangle area ratio, circle area ratio, square area, and center distance ratio" respectively. Subsequently, these extracted features are given as the input of the classification phase, in which the optimized NN is used. To make the detection more precise, the NN training is carried out by an optimization algorithm via tuning the optimal weights. For optimization purposes, this work deploys a new SAPSO algorithm. Thus, the presence or absence of the disease will be detected effectively. Fig. 1 illustrates the overall architecture of the adopted work.

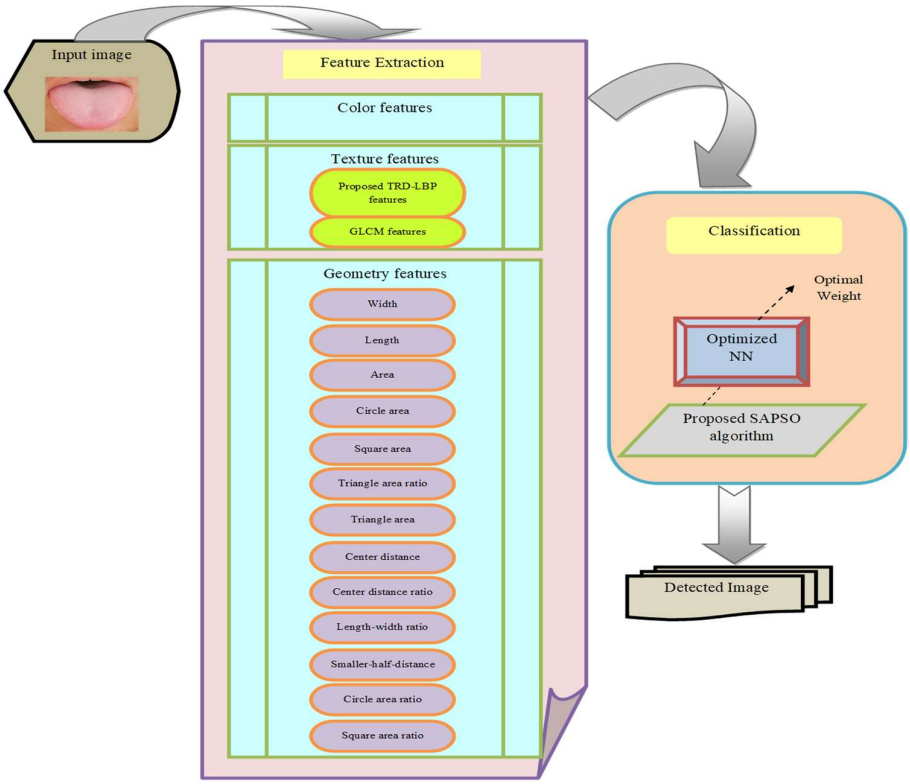

F*ig.2.The overall architecture of the adopted model*

Feature Extraction: Color Feature, Texture Feature, And Geometric Feature
The Feature Extraction Process Involves The Extraction Of Three Features That Include: (I) Color Feature, (Ii) Geometric Feature, And (Iii) Texture Feature.

3.2 Color Feature

All the feasible colors are symbolized in the tongue color gamut [34] that appears on the tongue surfaces, and exists in its boundary. Fig. 4 illustrates the 12 colors represented in the tongue color gamut with its labels. Furthermore, its CIELAB and RGB values are demonstrated in Table II.

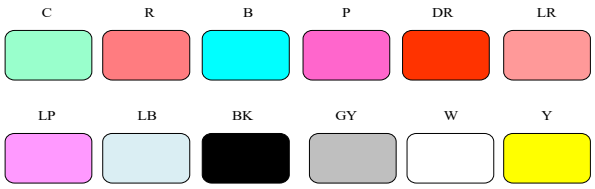

Fig.2.12 *Color representation of the tongue color gamut in its label.*

Table 2*. Clelab rgb values*

Color	[L A B]	[R G B]
Y (Yellow)	[56.3164 9.5539 24.4546]	[166 129 93]
LR (Light red)	[69.4695 28.4947 13.3940]	[227 150 147]
GY (Gray)	[61.6542 5.7160 3.7317]	[163 146 143]
P (Purple)	[69.4695 42.4732 -23.8880]	[226 142 214]
LB (Light blue)	[76.0693 7.8917 0.9885]	[204 183 186]
R (Red)	[52.2540 34.8412 21.3002]	[189 99 91]
W (White)	[70.9763 10.9843 8.2952]	[200 167 160]
DR (Deep red)	[37.8424 24.5503 25.9396]	[136 72 49]
BK (Black)	[37.8424 3.9632 20.5874]	[107 86 56]
B (Blue)	[69.4695 9.5423 -5.4951]	[183 165 180]
LP (Light purple)	[76.0693 24.3246 -9.7749]	[225 173 207]
C (Cyan)	[76.0693 -0.5580 1.3615]	[188 188 185]

The corresponding RGB values of a tongue image are extracted from the foreground pixels, and it is then converted into CIELAB [32] via transferring the RBG to CIEXYZ in Eq. (1). Moreover, the CIEXYZ is transferred to CIELAB as per Eq. (2).

$$\begin{bmatrix} X \\ Y \\ Z \end{bmatrix} = \begin{bmatrix} 0.4124 & 0.3576 & 0.1805 \\ 0.2126 & 0.7152 & 0.0722 \\ 0.0193 & 0.1192 & 0.9505 \end{bmatrix} \begin{bmatrix} R \\ G \\ B \end{bmatrix} \tag{1}$$

$$\begin{cases} L^* = 166.f\left(Y/Y_0\right) - 16 \\ a^{i*} = 500.\left[f\left(X/X_0\right) - f\left(Y/Y_0\right)\right] \\ b^* = 200.\left[f\left(Y/Y_0\right) - f\left(Z/Z_0\right)\right] \end{cases} \tag{2}$$

Where, $f(x) = x^{1/3}$ if $x > 0.008856$, or $f(x) = 7.787x + 16/116$ if $x \le 0.008856$.

In Eq. (2), the CIEXYZ tri-stimulus values are indicated as X_0, Y_0 and Z_0 of the white point reference. As per Table II, the 12 different colors from the color gamut of the tongue are compared with the LAB values and then assigned the color that is nearest to it, (i.e.), calculated using the Euclidean distance. Moreover, it summed the total colors and divided the entire pixels after evaluating all the foreground pixels from the tongue. The vector v of the tongue color feature is formed from the ratio of the 12 colors, here, c_i represents the sequence of colors, $v = [c_1, c_2, c_3, c_4, c_5, c_6, c_7, c_8, c_9, c_{10}, c_{11}, c_{12}]$. Moreover, the extracted color features are denoted as FE_{color}

3.3 Texture Feature

The texture feature includes both the proposed TRD-LBP feature and GLCM features.

Proposed TRD-LBP features: The distance based proposed TRD-LBP describes the distance between the consecutive neighbors. The center of the pixel is denoted as P_c and the $P = \{p_0, p_1, p_2, p_3, p_4, p_5, p_6, p_7, ...p_n\}$. Moreover, the proposed TRD-LBP features are extracted from three different regions: the pentagon, octagon, and heptagon regions.

$$S(p_i > p_j) = \begin{cases} 1 & , p_i > p_j \\ 0 & , p_i \le p_j \end{cases} \tag{3}$$

In Eq. (3), p_i is the initial pixel and p_j is its neighbor. *For pentagon region:* When distance $dist = 1$, the p_c can be computed as per Eq. (2). When, $dist = 2$, P_c is computed as per Eq. (5). When, $dist = 3$, P_c is computed as per Eq. (6).

$$P_c = \begin{Bmatrix} S(p_0 > p_1), S(p_1 > p_2), S(p_2 > p_3), \\ S(p_3 > p_4), S(p_4 > p_0) \end{Bmatrix} \tag{4}$$

$$P_c = \begin{Bmatrix} S(p_0 > p_2), S(p_1 > p_3), S(p_2 > p_4), \\ S(p_3 > p_0), S(p_4 > p_1) \end{Bmatrix} \tag{5}$$

$$P_c = \begin{Bmatrix} S(p_0 > p_3), S(p_1 > p_4), S(p_2 > p_0), \\ S(p_3 > p_1), S(p_4 > p_2) \end{Bmatrix} \tag{6}$$

For octagon region: When $dist = 1$, the p_c can be computed as per Eq. (7). When, $dist = 2$, P_c is computed as per Eq. (8). When, $dist = 3$, P_c is computed as per Eq. (9).

$$P_c = \begin{Bmatrix} S(p_0 > p_1), S(p_1 > p_2), S(p_2 > p_3), \\ S(p_3 > p_4), S(p_4 > p_5), S(p_5 > p_6), \\ S(p_6 > p_7), S(p_7 > p_0) \end{Bmatrix} \tag{7}$$

$$P_c = \begin{Bmatrix} S(p_0 > p_2), S(p_1 > p_3), S(p_2 > p_4), \\ S(p_3 > p_5), S(p_4 > p_6), S(p_5 > p_7), \\ S(p_6 > p_0), S(p_7 > p_1) \end{Bmatrix} \tag{8}$$

$$P_c = \begin{Bmatrix} S(p_0 > p_3), S(p_1 > p_4), S(p_2 > p_5), \\ S(p_3 > p_6), S(p_4 > p_7) S(p_5 > p_0), \\ S(p_6 > p_1), S(p_7 > p_2), \end{Bmatrix} \tag{9}$$

For Heptagon region: When $dist = 1$, p_c can be computed as per Eq. (10). When, $dist = 2$, P_c is computed as per Eq. (11). When, $dist = 3$, P_c is computed as per Eq. (12)

$$P_c = \begin{Bmatrix} S(p_0 > p_1), S(p_1 > p_2), S(p_2 > p_3), \\ S(p_3 > p_4), S(p_4 > p_5), S(p_5 > p_6), \\ S(p_6 > p_0) \end{Bmatrix} \tag{10}$$

$$P_c = \begin{Bmatrix} S(p_0 > p_2), S(p_1 > p_3), S(p_2 > p_4), \\ S(p_3 > p_5), S(p_4 > p_6), S(p_5 > p_0), \\ S(p_6 > p_1) \end{Bmatrix} \tag{11}$$

$$P_c = \begin{Bmatrix} S(p_0 > p_3), S(p_1 > p_4), S(p_2 > p_5), \\ S(p_3 > p_6), S(p_4 > p_0) S(p_5 > p_1), \\ S(p_6 > p_2) \end{Bmatrix} \tag{12}$$

The features extracted from the proposed TRD-LBP are denoted as FE^{lbp}. Fig. 3 illustrates the evaluation of the proposed TRD-LBP feature model.

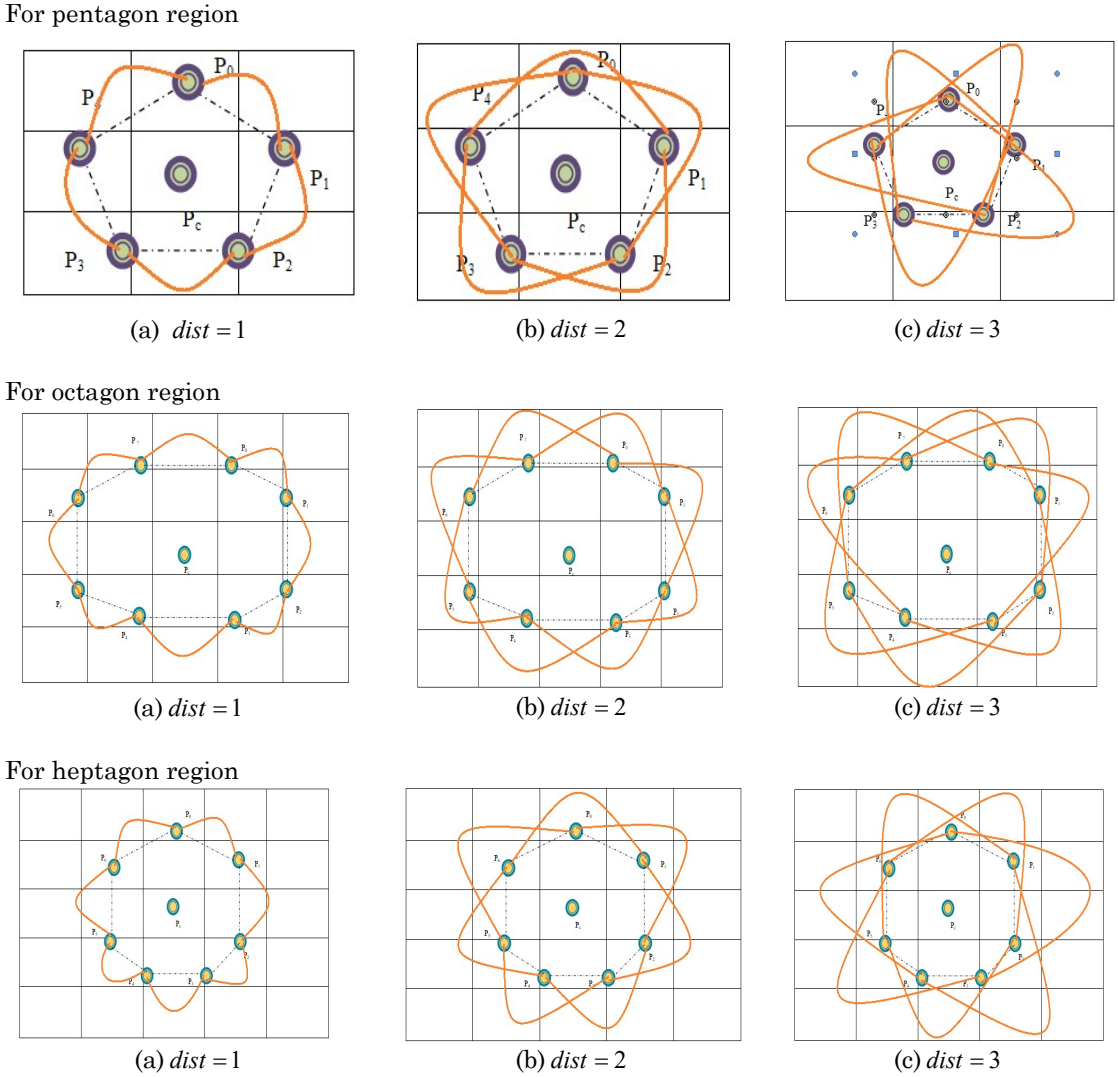

Fig.3.*Proposed TRD-LBP feature extraction*

GLCM Features: One of the familiar methods to gather the texture feature from the image is GLCM [35]. The extracted GLCM features are correlation, contrast, energy, homogeneity, mean, entropy, variance, SD, dissimilarity, cluster proximity, and maximum probability. Moreover, the count of elements in the matrix T and the dimension of the co-occurrence matrix M would assist in finding the features. Further, $J_{l,m}$ indicates the coordinates in the co-occurrence matrix using the term l,m.

Contrast is known as the 'Sum of Square Variance' and it is the difference between the brightness and the color of the image. Further, Eq. (13) depicts the arithmetic model for contrast measurement, if $l-m=0$, there exists no contrast in the image. The correlation is known as the measurement of the linear dependency of grey levels with its neighboring pixels in the image. The strain, displacement, deformation, and opaatical flowof the grey image are estimated by the correlation. Eq. (14) demonstrates the mathematical model for correlation, where, σ_l and σ_m indicates the SDs, and μ_l and μ_m specifies the mean of the pixel. Entropy is the measure of the quantity of information from the grey scale image needed for image compression. Eq. (15) illustrates the mathematical model for determining the entropy. The arithmetical formula for calculating the energyutilized in extending the repetition of pixel pair is described in Eq. (16). Homogeneity is the measure of tightness in the element distribution as in Eq. (17). Furthermore, the mean, variance, and standard deviation are calculated as per Eq. (18), Eq. (19) and Eq. (20), correspondingly. The term dissimilarity refers to the distance between the pairs of pixels as in Eq. (21).

$$Contrast = \sum_{l,m=0}^{T-1} J_{l,m}(l-m)^2 \tag{13}$$

$$Correlation = \sum_{l,m=0}^{T-1} J_{l,m}\left[\frac{(l-\mu_l)(m-\mu_m)}{\sqrt{\sigma_l^2.\sigma_m^2}}\right] \tag{14}$$

$$Entropy = \sum_{l,m=0}^{T-1}\left(-J_{l,m}\left(\log J_{l,m}\right)\right) \tag{15}$$

$$Energy = \sum_{l,m=0}^{T-1}\left(J_{l,m}\right)^2 \tag{16}$$

$$Homogenity = \sum_{l,m=0}^{T-1}\frac{J_{l,m}}{1+(l-m)^2} \tag{17}$$

$$Mean\ \mu_l = \sum_{l,m=0}^{T-1} l\left(J_{l,m}\right); \mu_m = \sum_{l,m=0}^{T-1} m\left(J_{l,m}\right) \tag{18}$$

$$\begin{aligned} Variance\ \ K_l &= \sum_{l,m=0}^{T-1} J_{l,m}\left(l-\mu_l\right); \\ K_m &= \sum_{l,m=0}^{T-1} J_{l,m}\left(m-\mu_m\right) \end{aligned} \tag{19}$$

$$SD\ \sigma_l = \sqrt{K_l^2}\ ;\ \sigma_m = \sqrt{K_m^2} \tag{20}$$

$$Dissimilarity = \sum_{l,m=0}^{T-1} J_{l,m}\left|l-m\right| \tag{21}$$

$$\max_{prob} = \max J_{l,m}\ \ for\ all\ values\ of\ l,m \tag{22}$$

$$clus_{prox} = \sum_{l,m=0}^{T-1}\left(l+m-\mu_m\right)^4 J_{l,m} \tag{23}$$

$$IDM = \sum_{l,m=0}^{T-1}\frac{1}{1+(l-m)^2}J_{l,m} \tag{24}$$

The maximum probability $\max_{prob}$ is defined as the measure of the higher probability of producing the pixels of interest and it is computed in Eq. (22). Furthermore, the cluster prominence is indicated as $clus_{prox}$ in which the clustering capability in ROI pixel is determined in Eq. (23). Moreover, the IDM of the grey scale image is given in Eq. (24). The extracted features from GLCM are indicated as FE^{glcm}. Moreover, Eq. (25) represents the final texture features.

$$FE_{texture} = FE^{lbp} + FE^{glcm} \tag{25}$$

3.4 Geometric Feature

From the tongue images, the 13 geometry features are extracted. Moreover, these geometric features are taken from the areas, distances, measurements, and their ratios.

Length: The length(L)feature is calculated as the vertical distance of the tongue's furthermost bottom edge$(y_{\max})$point along the y-axis to its furthermost top edge point$(y_{\min})$. Eq. (26) indicates the length features.

$$L = y_{\max} - y_{\min} \tag{26}$$

Width: The width (w) feature is calculated as the horizontal distance of the tongue's furthest right edge point $(x_{\max})$ along the x-axis to the furthest left edge point $(x_{\min})$. Eq. (27) specifies the width features.

$$w = x_{\max} - x_{\min} \tag{27}$$

Area: The entire foreground pixels of the tongue are known as the area (A) of a tongue.

Length-Width Ratio: (Lw) is calculated as the ratio of a tongue's length to its width, and it is expressed in Eq. (28), where, (Lw) indicates the length-width ratio.

$$Lw = L/w \tag{28}$$

Circle Area: (CA) is the present in the tongue foreground by the Z, here, $r = Z$, (CA) indicates the circle area.

Center Distance: (CD) is measured as the distance from $w's$ y-axis center point to its center point $l(y_c)$, and it is specified in Eq. (29), where, the center distance (CD).

$$CD = \frac{\left(\max\left(y_{x\max}\right) - \max\left(y_{x\min}\right)\right)}{2} - y_c \tag{29}$$

In Eq. (30), $y_c = \left(y_{\max} + y_{\min}\right)/2$.

Triangle Area: (TA) is described among the foreground of the tongue. Moreover, $x_{\max}$ is the triangle's right point, $x_{\min}$ is the triangle's left point, and $y_{\max}$ is the bottom, where, (TA) indicates the triangle area.

Circle Area Ratio: (CAR) is defined as the ratio of circle area (CA) to area (A), and it is mathematically expressed in Eq. (30).

$$CAR = \frac{CA}{A} \tag{30}$$

Smaller-Half-Distance: It is the half distance of L or w that depends on the shorter segment and is specified in Eq. (31), where, (Z) indicates the smaller-half-distance.

$$Z = \min\left(L, w\right)/2 \tag{31}$$

Square Area: (SA) is defined as the area of the square using Z smaller-half-distance that are defined within the tongue foreground, and it is described in Eq. (32), where, (SA) indicates the square area.

$$SA = 4Z^2 \tag{32}$$

Center Distance Ratio: (CDR) is measured as the ratio of center distance (CD) to length (L), and it is defined in Eq. (33).

$$CDR = \frac{CD}{L} \tag{33}$$

Triangle Area Ratio: It is defined as the ratio of triangle area (TA) to area (A), and it is represented in Eq. (34), where, (TAR) denotes the triangle area ratio.

$$TAR = \frac{TA}{A} \tag{34}$$

Square Area Ratio: (SAR) is defined as the ratio of Square area (SA) to area (A), and it is defined in Eq. (35).

$$SAR = \frac{SA}{A} \tag{35}$$

Moreover, the extracted geometric features are denoted as $FE_{geometric}$. Finally, the overall extracted features are expressed in Eq. (36).

$$FE = FE_{colour} + FE_{texture} + FE_{geometric} \tag{36}$$

4. Diabetes Mellitus Diagnosis via Optimized Neural Network

4.1 Optimized Neural Network

An NN is a series of algorithms that endeavors to recognize the fundamental relationships among the set of data by a process that imitates the way of human brain works. The input given to the NN [33] is the extracted features FE as specified in Eq. (37), where, n indicates the total features.

$$FE = \{FE_1, FE_2, ...FE_n\} \tag{37}$$

The NN framework consists of hidden, input, and output, layers. Moreover, the output in the hidden layer O is determined in Eq. (38), where, a denotes the "activation function", $\hat{f}$ and g refers to the neurons in the hidden layer and input layer respectively, $WE_{(v\hat{h})}^{(u)}$ indicating the bias weight with $\hat{f}^{th}$ hidden neuron, $\hat{Ne}_h$ specifies the input neurons count and $WE_{(g\hat{f})}^{(u)}$ denotes the weight among the input neuron g to the hidden neuron $\hat{f}$. Furthermore, the output of thenetwork $\hat{X}_z$ is determined in Eq. (39), where, H represents the number of hidden neurons, $WE_{(v\hat{z})}^{(X)}$ specifies theoutput bias weight of $\hat{z}^{th}$ the output layer, and thus $WE_{(\hat{f}\hat{z})}^{(X)}$ denotes the weight among the $\hat{f}^{th}$ hidden layers to z^{th} output layer. Consequently, the error that occurred in both predicted and actual values is determined in Eq. (40) which should be low. Eq. (40), Ne_D indicates the output neuron count $X_{\hat{z}}$ and $\hat{X}_{\hat{z}}$ denotes the actual and predicted output respectively.

$$O = a\left(WE_{(v\hat{f})}^{(u)} + \sum_{g=1}^{Ne\hat{f}} WE_{(g\hat{f})}^{(u)} In\right) \tag{38}$$

$$\hat{X}_{\hat{z}} = a\left(WE_{(v\hat{z})}^{(X)} + \sum_{\hat{f}=1}^{Neh} WE_{(\hat{f}\hat{z})}^{(X)} O\right) \tag{39}$$

$$Er^* = \underset{\left\{WE_{(v\hat{f})}^{(u)}, WE_{(g\hat{f})}^{(u)}, WE_{(v\hat{z})}^{(X)}, WE_{(\hat{f}\hat{z})}^{(X)}\right\}}{\arg\min} \sum_{z=1}^{NeD} \left|X_{\hat{z}} - \hat{X}_{\hat{z}}\right| \tag{40}$$

The NN model will be trained by a new SAPSO algorithm via optimizing the weights $WE = WE_{(v\hat{f})}^{(u)}, WE_{(g\hat{f})}^{(u)}, WE_{(v\hat{z})}^{(X)}, and\ WE_{(\hat{f}\hat{z})}^{(X)}$. Eq. (41) specifies the objective function of the adopted method intends to minimize the error.

$$Obj = \min\left(Er^*\right) \tag{41}$$

5. optimal tuning of weights via an improved particle swarm optimization algorithm

5.1 Proposed SAPSO Algorithm

Even though, the conventional PSO model offers better computational efficiency with satisfactory outcomes and robustness to control parameters; still, it falls easily into local optimum from the space which affects the optimization process. To overcome the drawbacks of the traditionalPSO model, the proposed SAPSO model intends to make some improvement to PSO that ensures better convergence and optimum results. Generally, self-improvement is established as a promising one in the existing optimization algorithms [26] [27] [28] [29] [30].The procedural steps are as follows:

Step 1: Initialize the position of the search agents as $Q = Q_1, Q_2, ..., Q_N$, and the velocity of the search agents as $E = E_1, E_2, \ldots, E_N$, where N indicates the count of search agents. Furthermore, the current iteration is indicated as I and $\max^I$ denotes the maximal iterations.

Step 2: While, $I < \max^I$ moving to step 3, else terminate.

Step 3: Calculate the fitness of the search agent using Eq. (41).

Step 4: The velocity update of d^{th} particle, $E_d(I+1)$ is given in Eq. (42).

$$E_d(I+1)=\omega E_d(I)+c_1 r_1\left(G_{qd}(I)-Q_d(I)\right)+ \\ +c_2 r_2\left(G_{bd}(I)-Q_d(I)\right) \tag{42}$$

In Eq. (13), r_1 and r_2 refers to the randomly distributed variables, and c_1 and c_2 indicates the acceleration coefficients, correspondingly. In addition, ω indicates the inertia weight, the local best and the global best toparticles are specified as $G_{bd}(I)$ and $G_{qd}(I)$, correspondingly. Moreover, the position update of the search agent is represented in Eq. (43).

$$Q_d(I+1)=Q_d(I)+E_d(I);\ \ d=1,2,..,F \tag{43}$$

As per the proposed logic, if the deciding factor $(im==1)$, the original PSO will be updated using Eq. (43) and assigned the variable $s=1$. Otherwise, the proposed update will be performed (that is given below) and then assigned $s=2$. Subsequently, check whether the current fitness is less than the previous fitness, if yes, then the deciding factor is assigned $im=s$, then the update will be performed accordingly. In the else case, it will update the position as per the condition $im=s$ set difference $(1{:}2, s)$.

The procedure of the proposed SAPSO update is as follows: Let us consider $Q=rand(lower\,bound, upper\,bound, CL)$, where, CL indicates the chromosome length. Moreover, the new variable (NV) can be found as $NV=rand(0,1,CL)$. If $index=find(NV==1)$, then

$$Q(index)=best(index) \tag{44}$$

Step 5: The boundaries of the search spaces are enforced based on the particle's position.
Step 6: Stop

The Algorithm 1 represents the pseudo-code of the adopted SAPSO model.

Algorithm 1: Adopted SAPSO Model
Initialize Q position of search agents
Initialize E velocity of search agents
While $I<\max^I$
Calculate the fitness of search agents in Eq. (39)
if $(im==1)$
Position update using Eq. (43)
Assign $s=1$
else
Position update using Eq. (44)
Assign $s=2$
end if
If $(Current\ fitness < previous\ fitness)$
$im=s$
else
$im=s$; Set diff(1:2, s)
end if
end while
Return

6. Results and Discussion

6.1 Simulation Procedure

The adopted NN+SAPSO model based DM detection was implemented using MATLAB and the resultant of each analysis was observed. The dataset was manually collected from 70 persons including 49 male and 21 female images of tongue samples. In addition, the betterment of the proposed DM detection method was compared to the existing models such as NN [33], SVM [34], and CNN [36] in terms of various measures like MCC, sensitivity, FNR, accuracy, FPR, specificity, NPV, precision, FDR, and F1-score, respectively. Here, the performance analysis is performed for different learning percentage that ranges from 50, 60, 70, and 80 respectively.

6.2 Performance Analysis

The performance analysis of the adopted method compared to the conventional schemes in terms of different measures is given in Fig. 4, 5, and 6 respectively. Further, the positive measures analysis is illustrated in Fig.4. On analyzing the graph, the positive measures like sensitivity, accuracy, precision,

and specificity of the proposed NN+SAPSO method show an improved outcome than other traditional models. Moreover, in Fig 4(c) the adopted NN+SAPSO model attains high accuracy for training percentage 70 than other existing schemes; specifically, the model is 12.76%, 29.78%, and 25.53% better than NN, SVM, and CNN models. In addition, the sensitivity of the adopted NN+SAPSO algorithm holds maximum values for training percentage 60 than other traditional models like NN, SVM, and CNN correspondingly, as given in Fig. 4(d). Similarly, the specificity of the proposed NN+SAPSO method as shown in Fig. 4(b) attains higher values (~1); however, the existing schemes like NN, SVM, and CNN hold the lowest values for training percentage 70. The proposed NN+SAPSO model has 15%, 35%, and 30% better precision values when compared to other traditional models like NN, SVM, and CNN respectively for training percentage 70 as in Fig. 4(a). Thus the betterment of the adopted NN+SAPSO method is proved.

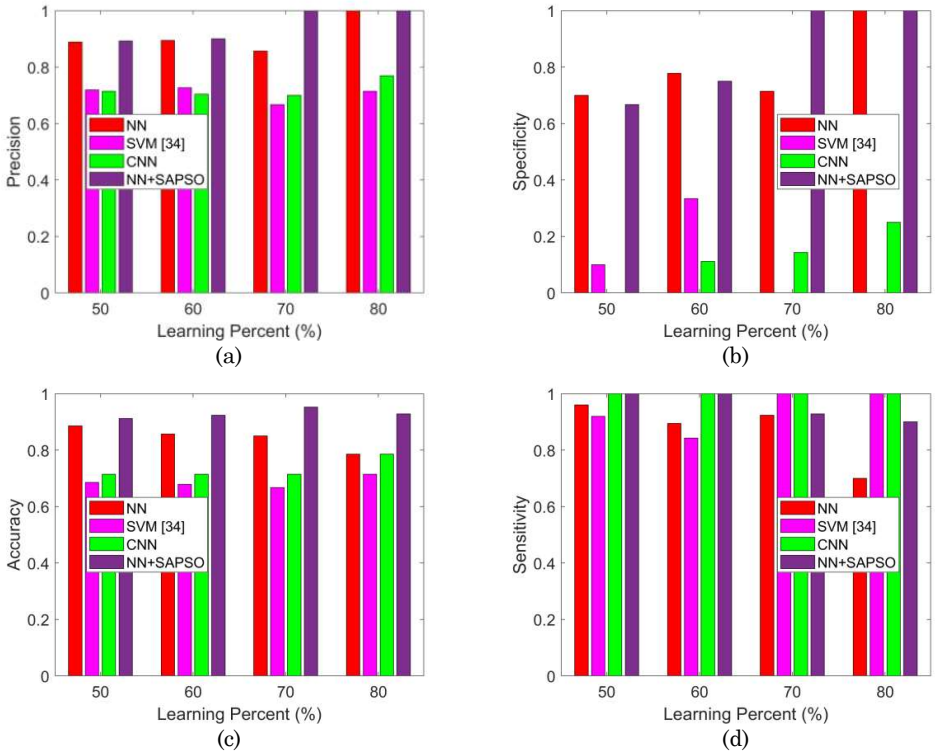

Fig.4.*Performance analysis of the adopted NN+SAPSOmethod over other existing schemes for (a) precision (b) specificity (c) accuracy (d) sensitivity*

The negative measures analysis like FDR, FNR, and FPR is illustrated in Fig. 5. For better performance, the negative measures should be lower. Likewise, the FPR of the implementedNN+SAPSO method for training percentage 50 is 61.11% and 65% better than the other conventional models such as SVM and CNN respectively in Fig. 5(a). The FNR of the proposed NN+SAPSO method holds a better value of (~0.1) for training percentage 80; whereas, the traditional NN modelholds the value of (~1) in Fig. 5(b). Further, the FDR of the proposed NN+SAPSO method achieves superior outcomes than other existing models like NN, SVM, and CNN respectively for training percentage 50 in Fig. 5(c). Thus, the improvement of the adopted NN+SAPSO model has proven effective.

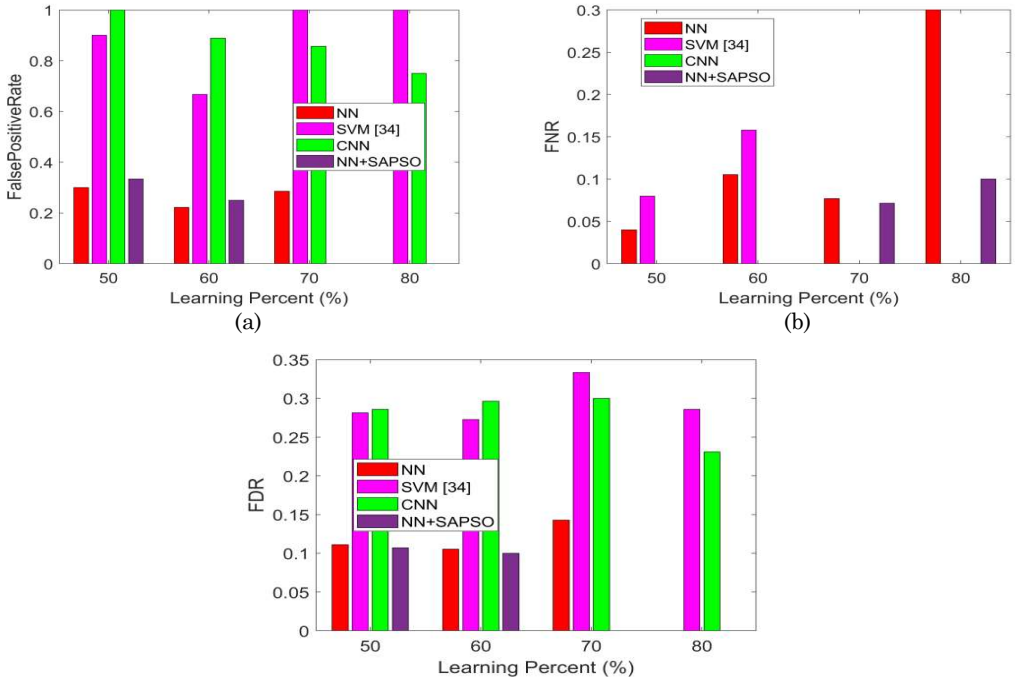

Fig.5. *Performance analysis of the adopted NN+SAPSOmethod over other existing schemes for (a) FPR (b) FNR (c) FDR*

Fig. 6 reveals the performance of other measures. From the graphs, it is observed that the NPV of the proposed NN+SAPSO method holds a value (~1) for training percentage 70, whereas the compared existing models like NN, SVM, and CNN attain lower NPV values in Fig. 6(a). However, in Fig 6(b), the F1-score of the adopted NN+SAPSO method for training percentage 60 than other existing models such as NN, SVM, and CNN shows an enhancement of 4.25%, 14.89%, and 12.76 % respectively. Similarly, the MCC of the presented NN+SAPSO model at training percentage 70 holds maximum values than the conventional models like NN, SVM, and CNN correspondingly. Finally, from the attained outputs it is clearly shown that the proposed NN+SAPSO method is superior to other traditional models in terms of various performance measures.

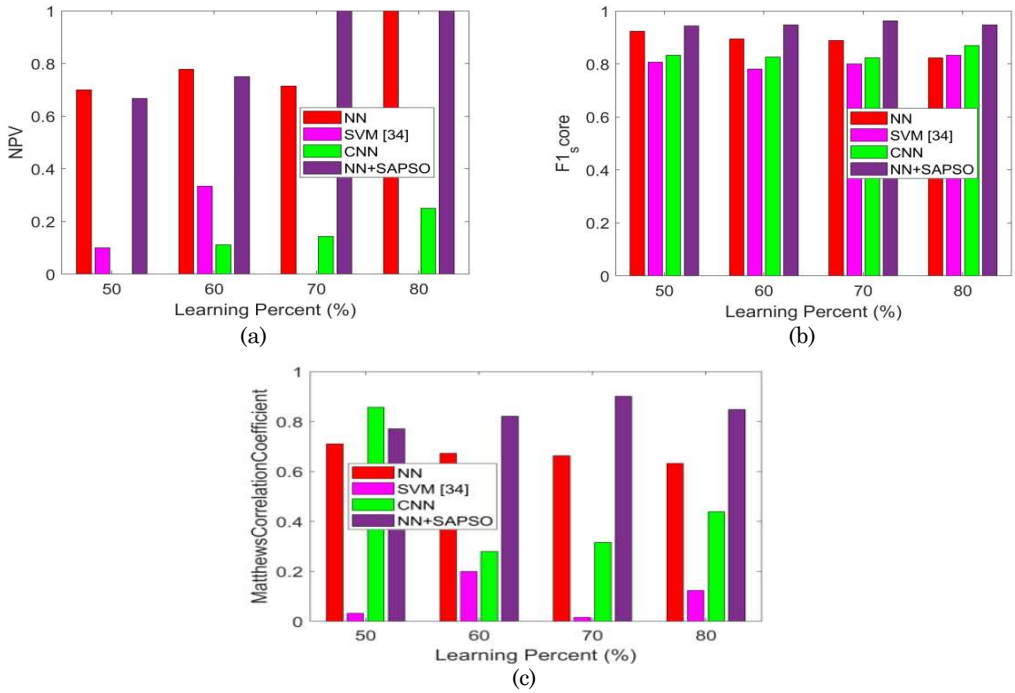

Fig.6. *Performance analysis of the adopted NN+SAPSO method over other existing schemes for (a) NPV (b) F1-score (c) MCC*

6.3 Error Analysis

The error analysis of the proposed NN+SAPSO method over the existing models like NN+FF, NN+JAYA, and NN+PSO is shown in Fig. 7. From the graphs, it is observed that the adopted NN+SAPSO method has attained better outcomes than other existing schemes with less error. Error analysis is carried out by varying the Epochs. Furthermore, the error analysis of the conventional NN+FF model holds the best validation performance of 0.5546 at epoch 2 in Fig. 7(a). Moreover, the error analysis of the conventional (i.e.) NN+JAYA model in Fig. 7(b) obtains the best validation performance of 0.026073 at epoch 1. The error analysis of the conventional NN+PSO model holds the best validation performance of 0.073949 at epoch 3 in Fig. 7(b). At last, the error analysis of the proposed NN+SAPSO method attains the best validation performance of 0.019391 (i.e.) minimum values at epoch 2 as illustrated in Fig. 7(d). While compared with the traditional models like NN+FF, NN+JAYA, and NN+PSO, the proposed NN+SAPSO method holds the minimum error performance, which shows the precise detection of DM.

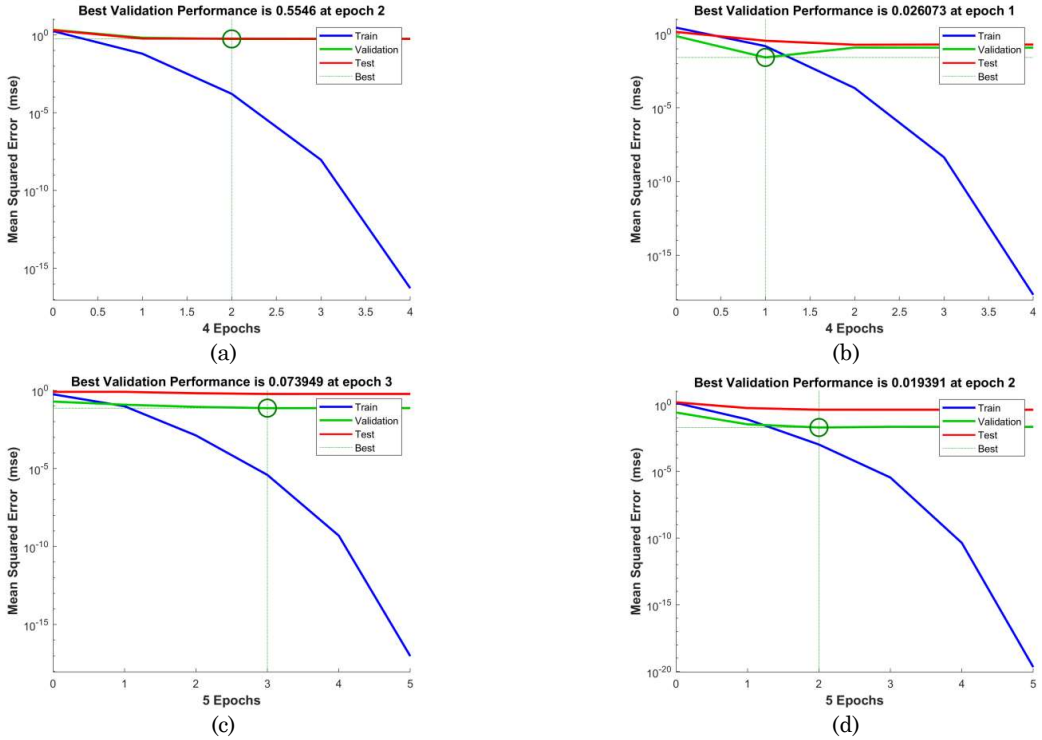

Fig.7.*Error analysis (a) NN+FF (b) NN+JAYA (c) NN+PSO (d) Proposed NN+SAPSO*

6.4 Performance Analysis by Learning Rate Variation

The overall performance analysis of the adopted NN+SAPSO scheme is compared to the existing models including NN+PSO[26], NN+FF [37], and NN+JAYA [38] for various measures by varying the learning rate as 50, 60, 70, and 80 respectively, and it is summarized in Table III, IV, V, and VI. On observing the table, the proposed NN+SAPSO model has proved its detection ability almost for all learning percent than other existing models like NN+PSO, NN+FF, and NN+JAYA, correspondingly. Similarly, the FNR, FPR, and FCR of the proposed NN+SAPSO method attain lower values for all learning rates than other traditional models. Similarly, the proposed NN+SAPSO model holds maximum values of MCC, F1-score, sensitivity, specificity, and precision for all the learning rates than other traditional models such as NN+PSO, NN+FF, and NN+JAYA correspondingly. Altogether, the analysis has proved the performance of the proposed work in the accurate detection of DM.

Table 3. *Comparative analysis of adopted and traditional models for learning percent 50*

Metrics	NN+PSO [26]	NN+FF [37]	NN+JAYA [38]	NN+SAPSO
Sensitivity	0.96	0.96	0.96	1
Accuracy	0.88571	0.88571	0.88571	0.91176
FDR	0.11111	0.11111	0.11111	0.10714
Specificity	0.7	0.7	0.7	0.66667
FPR	0.3	0.3	0.3	0.33333
MCC	0.71005	0.71005	0.71005	0.77152
FNR	0.04	0.04	0.04	0
NPV	0.7	0.7	0.7	0.66667
F1-score	0.92308	0.92308	0.92308	0.9434
Precision	0.88889	0.88889	0.88889	0.89286

Table 4. *Comparative analysis of adopted and traditional models for learning percent 60*

Metrics	NN+PSO [26]	NN+FF [37]	NN+JAYA [38]	NN+SAPSO
Sensitivity	0.89474	0.78947	0.94737	1
Accuracy	0.85185	0.82143	0.89286	0.92308
FDR	0.10526	0.0625	0.1	0.1
Specificity	0.75	0.88889	0.77778	0.75
FPR	0.25	0.11111	0.22222	0.25
MCC	0.64474	0.64019	0.74966	0.82158
FNR	0.10526	0.21053	0.052632	0
NPV	0.75	0.88889	0.77778	0.75
F1-score	0.89474	0.85714	0.92308	0.94737
Precision	0.89474	0.9375	0.9	0.9

Table 5. *Comparative analysis of adopted and traditional models for learning percent 70*

Metrics	NN+PSO [26]	NN+FF [37]	NN+JAYA [38]	NN+SAPSO
Sensitivity	0.85714	1	0.85714	0.92857
Accuracy	0.85714	0.85714	0.7619	0.95238
FDR	0.076923	0.17647	0.2	0
Specificity	0.85714	0.57143	0.57143	1
FPR	0.14286	0.42857	0.42857	0
MCC	0.69338	0.68599	0.44721	0.90139
FNR	0.14286	0	0.14286	0.071429
NPV	0.85714	0.57143	0.57143	1
F1-score	0.88889	0.90323	0.82759	0.96296
Precision	0.92308	0.82353	0.8	1

Table 6. *Comparative analysis of adopted and traditional models for learning percent 80*

Metrics	NN+PSO [26]	NN+FF [37]	NN+JAYA [38]	NN+SAPSO
Sensitivity	0.9	0.8	0.6	0.9
Accuracy	0.85714	0.85714	0.71429	0.92857
FDR	0.1	0	s0	0
Specificity	0.75	1	1	1
FPR	0.25	0	0	0
MCC	0.65	0.7303	0.54772	0.84853
FNR	0.1	0.2	0.4	0.1
NPV	0.75	1	1	1
F1-score	0.9	0.88889	0.75	0.94737
Precision	0.9	1	1	1

7. Conclusion

This paper has introduced a new DM diagnosis model that includes two major phases: (i) Feature extraction, and (ii) Classification. Initially, the input image was given to the feature extraction phase, in which the color feature, texture feature, and geometry features are extracted. The texture features include Proposed TRD-LBP and GLCM features, whereas, the 13 geometry features were also included in this feature extraction phase. Subsequently, these extracted features were provided as the input to the Optimized NN, where the diagnosis takes place. To make the detection more precise, the training of NN was carried out by a new SAPSO algorithm via tuning the optimal weights. Finally, the performance analysis was made among the adopted and the existing approaches to various measures like sensitivity, NPV, accuracy, FDR, specificity, FPR, precision, MCC, FNR, and F1-score respectively. On observing the

graph, the accuracy of the proposed NN+SAPSO method has attained superior outcomes for training percentage 70 than other existing schemes like NN, SVM, and CNN with 12.76%, 29.78%, and 25.53% respectively. In addition, the NPV of the proposed NN+SAPSO method holds a value (~1) for training percentage 70, whereas the compared existing models like NN, SVM, and CNN have attained lower NPV values. Moreover, the error analysis of the proposed NN+SAPSO method attains the best validation performance of 0.019391 (i.e.) minimum values at epoch 2. From the table, the proposed NN+SAPSO model has achieved higher accuracy for all learning percentages than other existing models like PSO, FF, and JAYA, respectively.

Compliance with Ethical Standards

Conflicts of interest: Authors declared that they have no conflict of interest.

Human participants: The conducted research follows the ethical standards and the authors ensured that they have not conducted any studies with human participants or animals.

References

[1] Biswas Anupam, Channabasappa, Shivaprasad, Sarathi Vijaya, Atluri Sridevi, Kumar Nikhil, "Prevalence of hypogonadism in patients with type 2 diabetes mellitus among the Indian population", Diabetes & Metabolic Syndrome: Clinical Research & Reviews, vol. 14, no. 5, pp. 1299-1304, Sept–Oct 2020.

[2] Rukiye Bozbulut, Nevin Şanlıer, Esra Döğer, Aysun Bideci, Peyami Cinaz, "The effect of beta-glucan supplementation on glycemic control and variability in adolescents with type 1 diabetes mellitus", Diabetes Research and Clinical Practice, vol. 169, Art. no. 108464, Nov 2020.

[3] Kusnanto Kusnanto, Hidayat ArifinIka Yuni, Widyawati, "A qualitative study exploring diabetes resilience among adults with regulated type 2 diabetes mellitus", Diabetes & Metabolic Syndrome: Clinical Research & Reviews, vol. 14, no. 6, pp. 1681-1687, Nov–Dec 2020.

[4] K. Kölle, T. Biester, S. Christiansen, A. L. Fougner, and Ø. Stavdahl, "Pattern Recognition Reveals Characteristic Postprandial Glucose Changes: Non-Individualized Meal Detection in Diabetes Mellitus Type 1," IEEE Journal of Biomedical and Health Informatics, vol. 24, no. 2, pp. 594-602, Feb. 2020, doi: 10.1109/JBHI.2019.2908897.

[5] Antonios Kousaxidis, Anthi PetrouVasiliki, Lavrentaki, Maria Fesatidou, Athina Geronikaki, "Aldose reductase and protein tyrosine phosphatase 1B inhibitors as a promising therapeutic approach for diabetes mellitus", European Journal of Medicinal Chemistry, vol. 207, Art. no. 112742, 1 Dec 2020.

[6] Brian J. KoosJeffrey A. Gornbein, "Early pregnancy metabolites predict gestational diabetes mellitus: implications for fetal programming", American Journal of Obstetrics and Gynecology, In press, corrected proof, Available online 31 July 2020.

[7] Masafumi Nozoe, Hiroki Kubo, Masashi Kanai, Miho Yamamoto, Kyoshi Mase, "Sarcopenia risk and diabetes mellitus are independent factors for lower limb muscle strength in elderly patients with acute stroke: A cross-sectional study", NutritionIn press, journal pre-proof, Art. no. 111025, Available online 18 Sept 2020.

[8] Achenef Asmamaw Muche, Oladapo O. OlayemiYigzaw Kebede Gete, "Gestational diabetes mellitus increased the risk of adverse neonatal outcomes: A prospective cohort study in Northwest Ethiopia", vol. 87, Art.no. 102713, Midwifery, Aug 2020.

[9] Beverly C. Tse, Barry Block, Heather Figueroa, Ruofan Yao, "Adverse neonatal outcomes associated with pregestational diabetes mellitus in infants born preterm", American Journal of Obstetrics & Gynecology MFM, In press, corrected proof, Available online, Art. no. 100213, 15 Aug 2020,

[10] B. Zhang, B. V. K. Vijaya Kumar, and D. Zhang, "Detecting Diabetes Mellitus and Nonproliferative Diabetic Retinopathy Using Tongue Color, Texture, and Geometry Features," IEEE Transactions on Biomedical Engineering, vol. 61, no. 2, pp. 491-501, Feb. 2014, doi: 10.1109/TBME.2013.2282625.

[11] Jiaojiao Tan, Haihong LvYuping Ma, Chunhua Liu, Chenyi Wang, "Analysis of angiographic characteristics and intervention of vitamin D in type 2 diabetes mellitus complicated with lower extremity arterial disease", Diabetes Research and Clinical Practice, vol. 169, Art. no. 108439, Nov 2020.

[12] Tri Sunaryo, Siti Lestari, Bibi, Florina, Abdullah, Sevendor, Khor, "The effect of oral hydrotherapy on risk reduction of diabetic feet ulcer among people with type-2 diabetes mellitus", Enfermería Clínica, vol. 30, Supplement 5, pp. 192-195, June 2020.

[13] Gyu S. Choi, Hye S. Min, Dae R. Cha, "SH3YL1 protein as a novel biomarker for diabetic nephropathy in type 2 diabetes mellitus", Nutrition, Metabolism and Cardiovascular Diseases, In press, corrected proof, Available online 25 Sept 2020.

[14] Mohamed Shawky Elsayed, Ayman El Badawy, Amr Mohamed, "Serum cystatin C as an indicator for early detection of diabetic nephropathy in type 2 diabetes mellitus", Diabetes & Metabolic Syndrome: Clinical Research & Reviews, vol. 13, no. 1, pp. 374-381, 28 Aug 2018 (Cover date: January–February 2019).

[15] Soorampally Vijay, Abdoul Hamide, Vadivelan Mehalingam, "Utility of urinary biomarkers as a diagnostic tool for early diabetic nephropathy in patients with type 2 diabetes mellitus" Diabetes & Metabolic Syndrome: Clinical Research & Reviews, vol. 12, no. 5, pp. 649-652, 12 April 2018 (Cover date: September 2018).

[16] Ioanna Theologia Lampropoulou, Maria Stangou, Aikaterini Papagianni, "TNF-α pathway and T-cell immunity are activated early during the development of diabetic nephropathy in Type II Diabetes Mellitus" Clinical Immunology, vol. 215, Art.no. 108423, 15 April 2020 (Cover date: June 2020).
[17] Dagfinn AuneYahya Mahamat-SalehTeresa NoratElio Riboli, "Diabetes mellitus and the risk of pancreatitis: A systematic review and meta-analysis of cohort studies", Pancreatology, vol. 20, no. 4, pp. 602-607, June 2020.
[18] Anjali Shrivastva, Sameer Phadnis, Karthik Rao N, Manisha Gore, "A study on knowledge and self-care practices about Diabetes Mellitus among patients with type 2 Diabetes Mellitus attending selected tertiary healthcare facilities in coastal Karnataka", Clinical Epidemiology and Global Health, vol. 8, no. 3, pp. 689-692, Sept 2020.
[19] Lori E. Arguello, Kasuen Mauldin, Deepika Goyal, "Patients With Prediabetes or Type 2 Diabetes Mellitus in a Medically Supervised Diet Program", The Journal for Nurse Practitioners, vol. 16, no. 8, pp. 612-616, Sep 2020.
[20] Saziya Bidi, D. C. Reshma, Shrimanjunath Sankanagoudar, "Comparison of urinary amino acid excretory pattern in patients with type 2 diabetes mellitus and non-diabetic healthy controls at a tertiary referral hospital in India", Diabetes & Metabolic Syndrome: Clinical Research & Reviews, vol. 14, no. 4, pp. 357-362, 13 April 2020, (Cover date: July–August 2020).
[21] Muhei Tanaka, Hiroshi OkadaYoshitaka Hashimoto, Muneaki Kumagai, Michiaki Fukui, "Low-attenuation muscle is a predictor of diabetes mellitus: A population-based cohort study", Nutrition, vol. 74, Art. no. 110752, June 2020.
[22] D. Sunil Kumar, B. Prakash, B. J. Subhash Chandra, Padma Shrinivas Kadkol, M. R. Narayana Murthy, "Technological innovations to improve health outcome in type 2 diabetes mellitus: A randomized controlled study", Clinical Epidemiology and Global Health, In press, corrected proof Available online 30 June 2020.
[23] Charupong, Saengboonmee, Wunchana, Seubwai, Worachart, Lert-itthiporn, Thanachai, Sanlung, Sopit, Wongkham, "Association of Diabetes Mellitus and Cholangiocarcinoma: Update of Evidence and The Effects of Anti-diabetic Medication", Canadian Journal of Diabetes, In press, journal pre-proof, Available online 17 Sept 2020
[24] Sanjib Sarkar, Dibyendu Das, Prachurjya Dutta, Jatin Kalita, Prasenjit Manna, "Chitosan: A promising therapeutic agent and effective drug delivery system in managing diabetes mellitus", Carbohydrate Polymers, Volume 247, Article 116594, November 2020.
[25] Merve Inanc, Kemal Tekin, Zehra Aycan, "Changes in Retinal Microcirculation Precede the Clinical Onset of Diabetic Retinopathy in Children With Type 1 Diabetes Mellitus" American Journal of Ophthalmology, vol. 207, pp. 37-44, 19 April 2019 (Cover date: November 2019).
[26] M.E.H.Pedersen and A.J.Chipperfield, "Simplifying Particle Swarm Optimization", Applied Soft Computing, vol. 10, no. 2, pp. 618-628, 2010.
[27] B. R. Rajakumar, "Impact of Static and Adaptive Mutation Techniques on Genetic Algorithm", International Journal of Hybrid Intelligent Systems, Vol. 10, No. 1, pages: 11-22, 2013, DOI: 10.3233/HIS-120161.
[28] B. R. Rajakumar, "Static and Adaptive Mutation Techniques for Genetic algorithm: A Systematic Comparative Analysis", International Journal of Computational Science and Engineering, Vol. 8, No. 2, pages: 180-193, 2013, DOI: 10.1504/IJCSE.2013.053087.
[29] S. M. Swamy, B. R. Rajakumar and I. R. Valarmathi, "Design of Hybrid Wind and Photovoltaic Power System using Opposition-based Genetic Algorithm with Cauchy Mutation", IET Chennai Fourth International Conference on Sustainable Energy and Intelligent Systems (SEISCON 2013), Chennai, India, Dec. 2013, DOI: 10.1049/ic.2013.0361.
[30] Aloysius George and B. R. Rajakumar, "APOGA: An Adaptive Population Pool Size based Genetic Algorithm", AASRI Procedia - 2013 AASRI Conference on Intelligent Systems and Control (ISC 2013), Vol. 4, pages: 288-296, 2013, DOI: https://doi.org/10.1016/j.aasri.2013.10.043.
[31] B. R. Rajakumar and Aloysius George, "A New Adaptive Mutation Technique for Genetic Algorithm", In Proceedings of IEEE International Conference on Computational Intelligence and Computing Research (ICCIC), pages: 1-7, December 18-20, Coimbatore, India, 2012, DOI: 10.1109/ICCIC.2012.6510293.
[32] H.Z. Zhang, K.Q. Wang, X.S. Jin, and D. Zhang, "SVR based color calibrat ion for tongue image," in Proc. International Conference on Machine Learning and Cybernetics, pp. 5065-5070, 2005.
[33] Yogeswaran Mohan, Sia Seng Chee, Donica Kan Pei Xin, and Lee Poh Foong, "Artificial Neural Network for Classification of Depressive and Normal in EEG", 2016 IEEE EMBS Conference on Biomedical Engineering and Sciences (IECBES), 2016.
[34] B. Zhang, B. V. K. Vijaya Kumar, and D. Zhang, "Detecting Diabetes Mellitus and Nonproliferative Diabetic Retinopathy Using Tongue Color, Texture, and Geometry Features," IEEE Transactions on Biomedical Engineering, vol. 61, no. 2, pp. 491-501, Feb. 2014, doi: 10.1109/TBME.2013.2282625.
[35] Z. Xing and H. Jia, "Multilevel Color Image Segmentation Based on GLCM and Improved Salp Swarm Algorithm," IEEE Access, vol. 7, pp. 37672-37690, 2019.
[36] Y. LeCun, K. Kavukvuoglu, and C. Farabet, "Convolutional networks and applications in vision", In Circuits and Systems, International Symposium on, pp.253–256, 2010.
[37] Hui Wang, Wenjun Wang, Xinyu Zhou, Hui Sun, Zhihua Cui, " Firefly algorithm with neighborhood attraction", Information Sciences, vol. 382–383, pp. 374-387, March 2017.
[38] R. Venkata Rao, "Jaya: A simple and new optimization algorithm for solving constrained and Unconstrained optimization problems", International Journal of Industrial Engineering Computations, vol. 7, pp.19-34, 2016.
[39] Cristin R, Gladiss Merlin N.R, Ramanathan L, Vimala S, "Image Forgery Detection Using Back Propagation Neural Network Model and Particle Swarm Optimization Algorithm", Multimedia Research, Vol.3, No.1, pp.21-32,2020.

[40] R. Cristin, Dr.V.Cyril Raj, and Ramalatha Marimuthu, "Face Image Forgery Detection by Weight Optimized Neural Network Model", Multimedia Research, Vol.2, No.2, pp.19-27,2019.
[41] Vasamsetti Srinivas, Santhirani Ch, "Hybrid Particle Swarm Optimization-Deep Neural Network Model for Speaker Recognition", Multimedia Research, Vol.3, No.1, pp.1-10,2020.
[42] Deepak Rewadkar and Dharmpal Doye, "Traffic-Aware Routing in Urban VANET using PSO Model", Journal of Networking and Communication Systems, Vol.2, No.2, pp.29-36,2019.
[43] Nitin Deotale, Uttam Kolekar, Anuradha Kondelwar, "Self-adaptive Particle Swarm Optimization for Optimal Transmit Antenna Selection", Journal of Networking and Communication Systems, Vol.3, No.1, pp.1-10,2020.
[44] Jyothi Mandala and Dr. M.V.P. Chandra SekharaRao, "HDAPSO: Enhanced Privacy Preservation for Health Care Data", Journal of Networking and Communication Systems, Vol.2, No.2, pp.10-19,2019.
[45] Vinolin V and S Vinusha, "Enhancement in Biodiesel Blend with the Aid of Neural Network and SAPSO", Journal of Computational Mechanics, Power System and Control, Vol.1, No.1, pp.11-17,2018.
[46] Gayathri Devi K.S, "Hybrid Genetic Algorithm and Particle Swarm Optimization Algorithm for Optimal Power Flow in Power System", Journal of Computational Mechanics, Power System and Control, Vol.2, No.2, pp.31-37,2019.